Supporting Information

Villares et al. 10.1073/pnas.1006886108

SI Materials and Methods

Cell Lines and Culture Conditions. The A375SM human melanoma cell line was maintained in modified Eagle medium supplemented with 10% FBS, as previously described (1). The C8161 and SB-2 human melanoma cell lines were maintained in DMEM-F12 supplemented with 5% FBS, as previously described (1, 2). The 293FT cells (Invitrogen) used to make lentiviral shRNA were maintained in DMEM supplemented with 10% FBS, per manufacturer's instructions.

Antibodies and Reagents. The PAR-1 antibody, ATAP2, used for FACS analyses was purchased from Santa Cruz Biotechnology. The PAR-1 antibody used for Western blot analyses was purchased from Immunotech Coulter. APC antibody was purchased from BioLegend. The PE (anti-mouse) antibody was purchased from Jackson ImmunoResearch. Anti-human Maspin antibody used for Western blots was purchased from BD Pharmingen. Ets-1, c-Jun, phospho c-Jun, c-Fos, phospho c-Fos, and IgG antibodies used for ChIP and Western blot assays were purchased from Santa Cruz Biotechnology. Phospho-p38, p38, and CBP/p300 antibodies were purchased from Cell Signaling Technology. Antibodies used for immunostaining include MMP-2 (Chemicon), Maspin (Abcam), VEGF (Santa Cruz Biotechnology), and goat anti-mouse or anti-rabbit HRP-IgG secondary antibodies (Jackson ImmunoResearch). The inhibitor of p38, SB 203580, was purchased from Calbiochem.

shRNA and siRNA. PAR-1 shRNA (target sequence, AGATTAGTCTCCATCAATA) and Maspin shRNA (target sequence, GGTGACACTGCAAATGAAAT), as well as an NT shRNA (target sequence, TTCTCCGAACGTGTCACGT), were used with the lentiviral system developed by Didier Trono as described previously (1). CBP/p300 siRNA (target sequence, AACCCCTCCTCUTCAGCACCA) was purchased from Dharmacon and transfected into PAR-1–silenced cells by using Hiperfect transfection reagent (Qiagen) per manufacturer's instructions.

Flow Cytometry. Flow cytometry was performed as previously described (1).

Western Blot Analysis. Maspin (1:1,000), phospho-p38 (1:1,000), p38 (1:1,000), and PAR-1 (1:250) were detected in total cell extracts by 10% SDS-polyacrylamide gel electrophoresis as we previously described (1). Ets-1, c-Jun, phospho-c-Jun, c-Fos, and phospho-c-Fos (1:1,000) were detected in nuclear extracts by using the Nuclear Extraction Kit from Panomics per manufacturer's instructions. CBP/p300 was detected in nuclear extracts by 8% SDS-polyacrylamide gel electrophoresis and transferred into an Immobilon-P transfer membrane (Millipore) using transfer buffer with 0.1% SDS overnight at 4 °C (30 V) followed by 1 h at room temperature at 100 V. The membranes were washed in Tris-buffered saline solution with Tween 20 (10 mm Tris·HCl, pH 8, 150 mm NaCl, and 0.05% Tween 20) and blocked with 5% nonfat milk in Tris-buffered saline solution with Tween 20 for 4 h. The blots were then probed overnight at 4 °C with primary antibody followed by 2 h of incubation with horseradish peroxide-conjugated secondary antibody. Immunoreactive proteins were detected by enhanced chemiluminescence using the ECL detection system per manufacturer's instructions (GE Healthcare). For Western blots using the p38 inhibitor, SB203580, cells were treated with 10 μM for 24 h before extracting protein, as previously described (3).

Semiquantitative RT-PCR. Semiquantitative RT-PCR was performed as previously described (1) using the following Maspin specific primers: forward, 5′-GCTTTTGCCGTTGATCTGTTC-3′; reverse, 5′-GATCTGACCTTTCGTTTTCTTC-3′.

cDNA Microarray. Microarray analysis was performed using the human Genome U133 Plus 2.0 Array (Affymetrix). The microarrays were produced in the microarray core facility of Codon Biosciences (Houston, TX). Total RNA was isolated from NT shRNA and PAR-1–silenced cells with the RNAquesous kit (Ambion) according to the manufacturer's instructions. The data were analyzed by Codon Biosciences. Raw data have been deposited in the Gene Expression Omnibus database (accession no. GSM596624).

Reporter Constructs and Luciferase Activity Assays. The Maspin promoter region (−1.1 kb to +83 bp from the transcription initiation site) was amplified from C8161 genomic DNA using the following primers: forward, 5′-GGGGTACCGACTGCATACTGTACATCAGGTCTG-3′; reverse, 5′-CCGCTCGAGGCAGCGGTGGCTCACCTGGGCAGC-3′. The fragment was digested with KpnI and XhoI and ligated into the pGL3-basic vector (Promega). Site-directed mutagenesis for Ets-1 elements was performed by two nucleotide substitutions (italic) in the Ets-1 binding motif (CTTCCT to C*G*TC*G*T) to create mutations as described previously (4): Ets-1 (−476) 5′-GATTTTAAAAAGAAAC*G*TC*G*TGCGCCACCCATTAAAC -3′; Ets-1 (−115), 5′-GTA-ACTCACAGCCCC*G*TC*G*TGCCCGAACATGTTGGAGG -3′.

The AP-1 binding site at position −54 was mutated from TGAATCA to *A*CAA*C*AA (5), whereas the AP-1 site at position −510 was mutated from TGAGTAA to *G*GA*C*TAA as previously described (6, 7): AP1 (−510), 5′-GCCACCGCGCCAGGCC*G*GA*C*TAATCCTAATCACAGG -3′; AP1 (−54), 5′-CAGTAACTTCAGCC*A*CAA*C*AATTTCTTTCAATTGTG-3′.

Transient transfections of these constructs were performed using Lipofectin (Invitrogen) according to the manufacturer's instructions. A total of 2.5×10^4 cells per well in a 24-well plate were transfected with 0.5 μg of the pGL3-basic expression vector with no promoter or enhancer sequence, with 0.5 μg of pGL3-Maspin or pGL3-Maspin-mutant firefly luciferase expression constructs. For each transfection, 2.5 ng of CMV-driven renilla luciferase reporter construct (Promega) was included. After 6 h, the transfection medium was replaced with serum-containing growth medium. After 72 h, the cells were harvested and subjected to lysis, and the luciferase activity was assayed by using a Dual Luciferase Reporter Assay System (Promega) according to the manufacturer's instructions. The luciferase luminescence (relative light intensity $\times 10^6$) was measured with the LUMIstar reader (BMG Labtech). The ratio of firefly luciferase activity to CMV-driven renilla luciferase activity was used to normalize for differences in transfection efficiency among samples.

Maspin Expression Vector. A 1.2-kb region of the Maspin ORF was amplified from C8161 genomic DNA using the following primers: forward, 5′-CATATGGATGCCCTGCAACTAGCAAATTC-3′; reverse, 5′-TTAAGGAGAACAGAATTTGCCAAAG-3′. The PCR was performed using PfuUltra Hotstart PCR Master Mix (Stratagene). The PCR product was run on an agarose gel, the appropriate band was cut, and the DNA was purified by using the Geneclean Spin Kit (Qbiogene). The purified Maspin DNA was cloned into pcDNA4/HisMax Topo expression vector (Invitrogen) according to the manufacturer's protocol. For stable transduction of the Maspin expression vector, the insert was

digested from the pcDNA4 expression vector with MluI followed by blunt ending and a second digestion with XhoI. The DNA was recovered after running product on an agarose gel and purifying the DNA. The Maspin insert was then ligated into the pLVX-DsRed-Monomer-C1 vector using XhoI.

Immunohistochemistry. Formalin-fixed, paraffin-embedded sections were deparaffinized by sequential washing with xylene and graded ethanol (100%, 95%, 80%) and rehydrated in PBS solution. Antigen retrieval was done by heating in a steam cooker in 1× Target Retrieval Solution (Dako) for 20 min. After cooling and washing with PBS solution, endogenous peroxide was blocked with 3% hydrogen peroxidase inhibitor in PBS solution for 12 min. Nonspecific proteins were blocked in 5% horse serum and 1% goat serum for 20 min. Slides were incubated with MMP-2 polyclonal antibody (1:400) and Maspin antibody (1:200) overnight at 4 °C. Slides were washed, incubated for 10 min in protein-blocking solution, and reacted with goat anti-mouse or goat anti-rabbit HRP-IgG secondary antibodies (1:500) for 1 h at room temperature. Signal was detected with 3,3′-diaminobenzidine (Phoenix Biotechnologies) substrate for 6 min and counterstained with Gill no. 3 hematoxylin (Sigma) for 20 s. VEGF was analyzed by immunohistochemistry as we previously described (1).

1. Villares GJ, et al. (2008) Targeting melanoma growth and metastasis with systemic delivery of liposome-incorporated protease-activated receptor-1 small interfering RNA. *Cancer Res* 68:9078–9086.
2. Chen EI, Yates JR (2006) Maspin and tumor metastasis. *IUBMB Life* 58:25–29.
3. Trevino JG, et al. (2005) Expression and activity of SRC regulate interleukin-8 expression in pancreatic adenocarcinoma cells: Implications for angiogenesis. *Cancer Res* 65:7214–7222.
4. DeKoter RP, et al. (2007) Regulation of the interleukin-7 receptor alpha promoter by the Ets transcription factors PU.1 and GA-binding protein in developing B cells. *J Biol Chem* 282:14194–14204.
5. Oeth P, Parry GC, Mackman N (1997) Regulation of the tissue factor gene in human monocytic cells. Role of AP-1, NF-kappa B/Rel, and Sp1 proteins in uninduced and lipopolysaccharide-induced expression. *Arterioscler Thromb Vasc Biol* 17:365–374.
6. Bao BY, Yeh SD, Lee YF (2006) 1alpha,25-dihydroxyvitamin D3 inhibits prostate cancer cell invasion via modulation of selective proteases. *Carcinogenesis* 27:32–42.
7. Clark IM, et al. (1997) Transcriptional activity of the human tissue inhibitor of metalloproteinases 1 (TIMP-1) gene in fibroblasts involves elements in the promoter, exon 1 and intron 1. *Biochem J* 324:611–617.

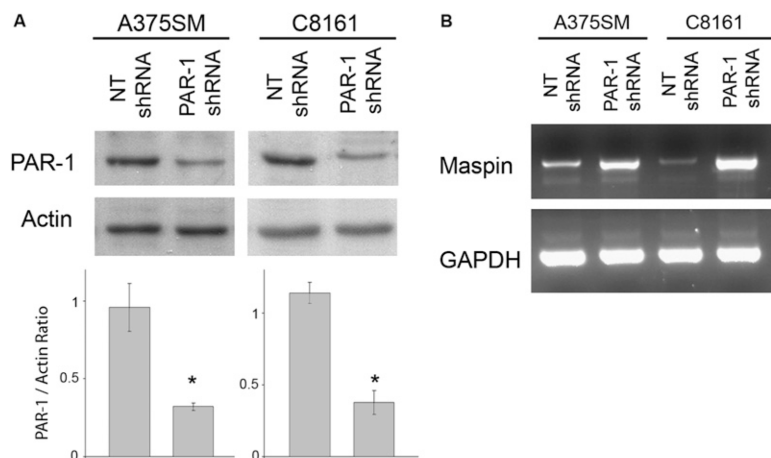

Fig. S1. Stable silencing of PAR-1 in metastatic melanoma cell lines and its effect on Maspin expression. (*A*) Western blot analyses demonstrate a significant decrease in PAR-1 protein expression after stably silencing two metastatic melanoma cell lines with PAR-1 shRNA. Data are presented as means ± SD from three independent experiments (*$P < 0.001$). (*B*) Semiquantitative RT-PCR demonstrates an increase in Maspin mRNA levels after stably silencing PAR-1 in two metastatic melanoma cell lines.

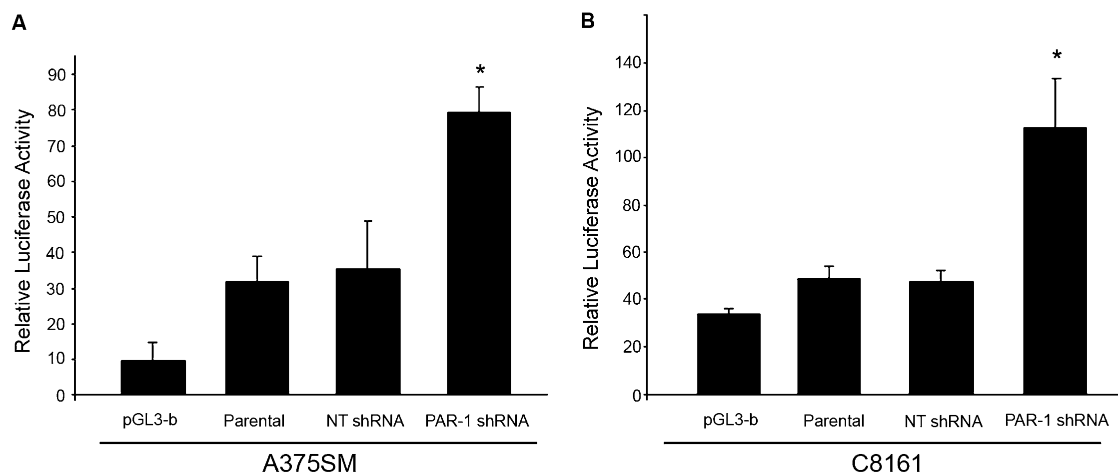

Fig. S2. Transcriptional regulation of Maspin promoter in PAR-1–silenced metastatic melanoma cell lines. The luciferase activity driven by the Maspin promoter was significantly increased by PAR-1 silencing in both (*A*) A375SM and (*B*) C8161 cell lines compared with NT-transduced cells. The ratio of firefly luciferase activity to CMV-driven renilla luciferase activity was used to normalize for differences in transfection efficiency among samples (*$P < 0.001$). Data are presented as means ± SD from three independent experiments.

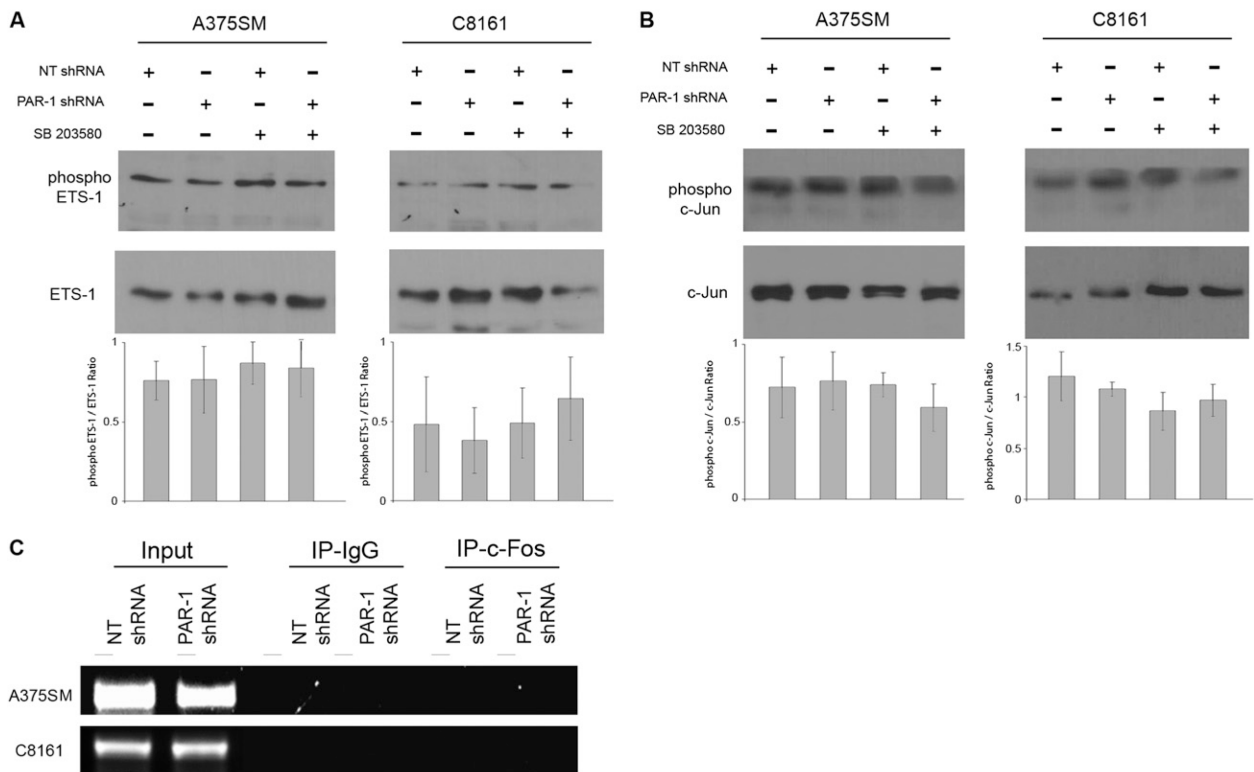

Fig. S3. Effects of inhibiting PAR-1 and phospho p38 on AP-1 and Ets-1 expression. No significant differences are seen in either phospho- or total protein levels of (*A*) Ets-1 or (*B*) c-Jun after PAR-1 silencing or after inhibiting phospho-p38 using SB 203580. Data are presented as means ± SD from three independent experiments. (*C*) ChIP studies failed to detect binding of c-Fos to the Maspin promoter in PAR-1–silenced cell lines or NT-transduced cells. Input DNA is used to determine equal amounts of chromatin in each condition used.

Fig. S4. Effects of Ets-1 and AP-1 transcription factor binding site mutations on Maspin promoter activity in PAR-1–silenced metastatic melanoma cell lines. Nonmutated Maspin promoter activity is increased after PAR-1 silencing in A375SM and C8161 melanoma cell lines ($P < 0.001$). Mutating the proximal Ets-1 site completely abrogated these effects in both cell lines. Mutating AP-1 at position −54 also reduced Maspin expression in PAR-1–silenced cells but to a lesser degree than with the Ets-1 (−115) mutation in both cell lines. The distal Ets-1 or AP-1 sites did not affect Maspin promoter activity in C8161 cell lines and minimally in A375SM. Data are presented as means ± SD from three independent experiments (**$P < 0.05$, *$P < 0.001$).

Fig. S5. Densitometry of phospho-p38 expression after PAR-1 silencing. A significant difference in phospho-p38 protein expression is seen by densitometry analysis after PAR-1 silencing in both metastatic melanoma cell lines (*$P < 0.001$). Data presented as mean ± SD from three independent experiments.

Fig. S6. Phospho-p38 and CBP/p300 regulate Maspin expression levels in metastatic melanoma cell lines. (*A*) Western blot analyses depict a significant decrease in phospho-p38 protein levels in PAR-1–silenced cells compared with NT shRNA-transduced cells. (**P* < 0.01). Using the p38 inhibitor, SB 203580, NT shRNA-transduced cells now show decreased levels of phospho-p38 (**P* < 0.001). (*B*) Densitometry analyses depict a significant increase in CBP/p300 protein levels after using the p38 inhibitor (SB 203580) in NT-transduced metastatic melanoma cell lines (**P* < 0.001). (*C*) Western blot analyses depict a significant decrease in CBP/p300 protein levels after transfecting PAR-1–silenced cells (i.e., high CBP/p300 expressors) with CBP/p300 siRNA (**P* < 0.001). (*D*) Densitometry from Western blot analyses depict a significant decrease in Maspin protein expression after using CBP/p300 siRNA on PAR-1–silenced cells (i.e., high Maspin expressors; ***P* < 0.01). (*E*) Increased Maspin expression is seen in NT shRNA-transduced cells after decreasing phospho-p38 using SB 203580 (**P* < 0.001). Data from all experiments are presented as mean ± SD from three independent experiments.

Fig. S7. Re-expressing PAR-1 using a nontargetable PAR-1 expression vector in A375SM and C8161 metastatic human melanoma cell lines. (*A*) A375SM and C8161 melanoma cell lines were transduced with a nontargetable PAR-1 expression vector (seven silent point mutations are present in the ORF of the PAR-1 sequence targeted by the stably transduced PAR-1 shRNA). Both cell lines show an increase in PAR-1 expression after PAR-1 rescue (orange) compared with PAR-1–silenced cells transduced with an EV control (red). APC and PE intensity (*Insets*) indicate PAR-1 expression. Representative images from three independent experiments are shown. (*B*) Densitometry from Western blot depict a significant decrease in Maspin expression after PAR-1 is restored in PAR-1–silenced metastatic melanoma cell lines (*$P < 0.001$, **$P < 0.01$). (*C*) Western blot depicting a significant decrease in Maspin protein expression when PAR-1 is transduced into a low PAR-1–expressing nonmetastatic melanoma cell line, SB-2 (*$P < 0.001$). Data presented as mean ± SD from three independent experiments.

Fig. S8. Effects on invasion after expressing Maspin in metastatic melanoma cell lines. (*A*) Western blot depicts A375SM and C8161 metastatic melanoma cells transduced with a Maspin expression vector having significantly higher levels of Maspin protein expression compared with cells transduced with EV control ($P < 0.001$). (*B*) Maspin-transduced A375SM and C8161 cell lines had a significant decrease in invasive capability when using a Matrigel chamber compared with cells transduced with an EV control ($*P < 0.01$). Data are presented as means ± SD from three independent experiments. (*C*) Zymography assay depicts decreased MMP-2 activity in both A375SM and C8161 cells transduced with a Maspin expression vector compared with EV control (i.e., low Maspin expressors). FBS 1% is used as a positive control. As a negative control, serum-free medium was used.

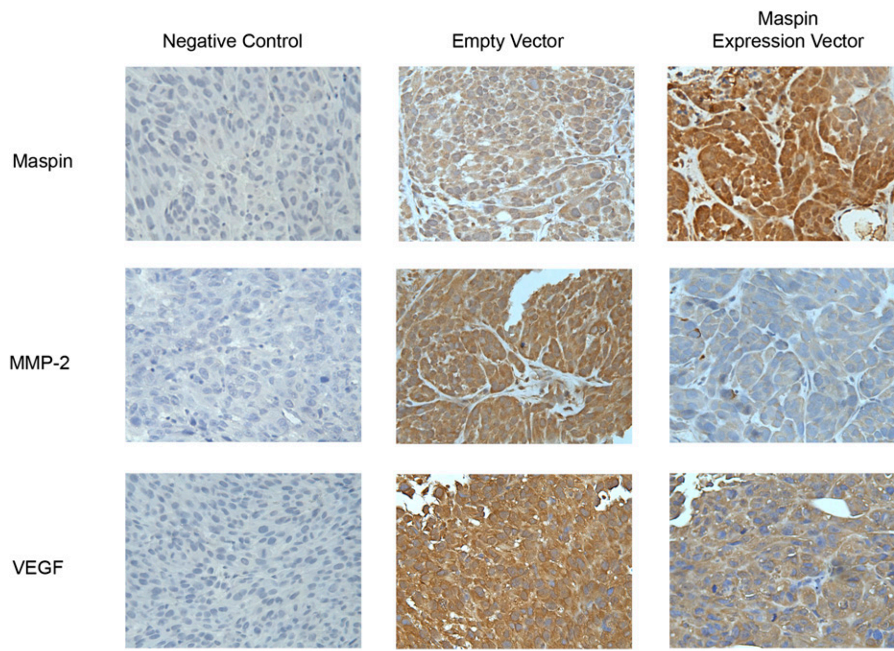

Fig. S9. In vivo effects of Maspin in melanoma. Tumors arising from A375SM metastatic melanoma cells stably transduced with Maspin or with an EV control were harvested and analyzed by IHC for Maspin and MMP-2 expression as well as VEGF. Tumors from mice injected with Maspin-expressing A375SM cells had increased Maspin expression along with decreased MMP-2 and. VEGF levels. Images are shown at 20× magnification.

Fig. S10. Effects of silencing Maspin in PAR-1–silenced cells. (*A*) Western blot depicts a significant decrease in Maspin protein expression levels in PAR-1–silenced cells (i.e., high Maspin expressors) after stable transduction with Maspin shRNA in two metastatic melanoma cell lines (*$P < 0.001$). Data are presented as means ± SD from three independent experiments. (*B*) Tumors from A375SM metastatic melanoma cells stably transduced with NT shRNA, PAR-1 shRNA, or PAR-1 shRNA plus Maspin shRNA were harvested and analyzed by IHC. Tumors arising from A375SM transduced with PAR-1 shRNA and Maspin shRNA show increased MMP-2 and VEGF levels compared with PAR-1–silenced cells alone. Images are shown at 20× magnification.